International Journal of Automotive Technology, Vol. 6, No. 6, pp. 607–613 (2005)

1229-9138/2005/024-08

APPLICATION OF VISCOELASTIC DAMPING FOR PASSIVE VIBRATION CONTROL IN AUTOMOTIVE ROOF USING EQUIVALENT PROPERTIES

K. H. LEE[1)*] and C. M. KIM[2)]

[1)]Hyundai Motor Co., 772-1 Jangduk-dong, Hwaseong-si, Gyeonggi 445-706, Korea
[2)]Graduate School of Automotive Engineering, Kookmin University, Seoul 136-702, Korea

(Received 19 August 2004; Revised 5 August 2005)

ABSTRACT–In this study, a simplified approach to modeling the dynamic characteristics of passive constrained layer damping treatments in finite element models is presented. The basic concept is to represent multi-layered composite structures using an equivalent single layer. The equivalent properties are obtained by using the RKU (Ross, Kerwin and Ungar) equations. Comparisons are given between results obtained by the dynamic analysis of the simple models implemented in MSC/NASTRAN and by test measurements. Surface damping treatments are applied to automotive panels as well as simple structures. Using the proposed equivalent modeling technique, higher computational efficiency for the damped composite structures has been obtained.

KEY WORDS : Damping, Viscoelastic material, Equivalent properties, Finite element analysis

1. INTRODUCTION

The noise, vibration and harshness (NVH) performance plays a critical role for emotional field in the design of vehicle Body-In-White (BIW) structures rather than other design parameters such as durability and crashworthiness. Reduction of interior noise and vibration is a major requirement for achieving world-class vehicle quality, performance and customer satisfaction. High power engine and light weighting to improve fuel economy are responsible for interior noise induced from the structure-borne-noise as main sound source, especially booming noise of lower frequency ranges (50 Hz–300 Hz) in the automobile.

Surface damping treatments are often used to solve a variety of interior noise and vibration in passenger vehicles. Such treatments can easily be applied to existing structures and provide high damping capability over wide temperature and frequency range. The surface damping treatments are largely classified in one of two categories, according to whether the damping material is subjected to extensional or shear deformation. Free layer damping type which is a layer of damping material added to the surface of the base structure attenuates vibration energy by longitudinal contractions and extensions to heat energy. On the other hand, constrained layer damping type which consists of a sandwich of two outer elastic layers with a viscoelastic material as the core refers to the extraction of shear energy from vibratory energy by conversion into heat (Mashif, 1985; Mead, 2000). Global body modes in low frequency range are not affected by the localized effects of damping treatments. Therefore the stiffness and damping effects of these treatments may be consequently ignored. However, at higher frequencies (beyond–300 Hz) body panel modes begin to appear and localized effects of damping treatments can no longer be ignored. Therefore, in some cases it may be important to include the effect of damping treatments in the FE models. The properties of viscoelastic core material in commonly used damping treatments exhibit a strong dependence on frequency and temperature. The applied treatments also significantly change the dynamic characteristics of the base system. Therefore, in order to accurately capture the dynamics of these treatments, the details of the damping layers, as well as their frequency and temperature dependent material properties must be included in the FE models. In the detailed model construction, the base panel, the viscoelastic core material and the constraining layer can be modeled with 3D solid elements. Such an approach requires considerable modeling effort. Most importantly, this results in a very large model, which may be expensive or even impossible to solve since the FE models already have a large number of degrees of freedom. Hence, it is a

**Corresponding author.* e-mail: predawn@hyundai-motor.com

necessity to explore other possibilities. One alternative to detailed modeling is to simulate such a complex multi-layer system, which the damping layers is attached on the base panel in an efficient and effective manner, with a single shell element that gets equivalent properties (Akanda and Goetchius, 1999; Wang, 1999). The analysis technigues for predicting the frequency response function (FRF) of damped automotive panels by use of equivalent shell element implemented in dynamic analysis from MSC/NASTRAN are developed.

2. BEHAVIOR OF VISCOELASTIC MATERIALS

For elastic materials that can be modeled by a spring, the shearing stress occurs in phase with the strain as shown in Figure 1(left).

On the other hand, for viscous materials that can be modeled by a dashpot, the shearing stress is 90° out of phase with the strain, as illustrated in Figure 1 (middle). That is to say, the strain occurs some time after the stress is applied. In the case of a viscoelastic material, the effects represented by the elastic element and the viscous element are combined. They relate the in-phase and quadrature-phase components of dynamic stress to the dynamic strain in time. As shown in Figure 1 (right), dynamic stress is a little leading the dynamic strain. As aforementioned relation can be written as follows:

$$\gamma(t) = \gamma_0 \cos \omega t \tag{1}$$

$$\sigma(t) = \sigma_0[\cos\delta\cos\omega t - \sin\delta\sin\omega t] \tag{2}$$

It follows from (2) that the stress amplitude per the strain amplitude is

$$G^* = G_1 + iG_2 = G_1(1 + i\tan\delta) \tag{3}$$

where

$$G_1 = \sigma_0\cos\delta/\gamma_0$$

$$G_2 = \sigma_0\sin\delta/\gamma_0$$

$$\eta = \tan\delta = G_2/G_1$$

G^* is complex modulus of elasticity, δ is the loss angle, G_1 is the storage modulus of elasticity, G_2 is the loss modulus of elasticity and η is the loss factor. In accordance with these quantities represented the dynamic characteristics

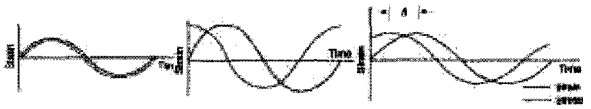

Figure 1. Stress and strain vs. time in dynamic loading of elastic (left), viscous (middle), and viscoelastic elements (right).

of viscoelastic material, some behaviors in viscoelastic materials are as follows:

(a) if the stress is held constant, the strain increases with time; (b) if the strain is held constant, the stress decreases with time (relaxation); (c) the effective stiffness depends on the rate of application of the load; (d) if cyclic loading is applied, hysteresis (a phase lag) occurs, leading to a dissipation of mechanical energy; (e) acoustic waves experience attenuation; (f) rebound of an object following an impact is less than 100%; (g) during rolling, frictional resistance occurs.

3. MATHEMATICAL MODELING

Since the focus of this paper is the single or double layered damping treatments commonly used in the automotive industry, the RKU equation which is usually used to handle both extensional and shear types of treatment was employed in this study. This equation has accuracy, simplicity and ease of use so that it is the most widely used method for the equivalent bending rigidity and loss factor calculation of panels treated with three layer damping treatments (Ross *et al.*, 1959). In order to extract the properties of viscoelastic core, it is a common practice to employ Oberst bar tests as specified by ASTM E756 (ASTM E756, 1993). However it may be quite expensive in practice, when a large number of bars have to be tested. The SAE J1637, on the other hand, is convenient and desirable to realize the same boundary condition as for certain types of automotive constrained layer damping treatments on account of the aymmetric configuration (SAE J-1637, 1993). Hence the ASTM equations accommodated for asymmetric Oberst bar configurations for sandwiched bars are modified to extract the properties of viscoelastic core (Akanda and Onsay, 2003).

The flexural rigidity, EI, of the three layer system of Figure 2 is:

$$\begin{aligned} EI = {} & E_1\frac{H_1^3}{12} + E_2\frac{H_2^3}{12} + E_3\frac{H_3^3}{12} - E_2\frac{H_2^3}{12}\left(\frac{H_{31}-D}{1+g}\right) \\ & + E_1H_1D^2 + E_2H_2(H_{21}-D)^2 + E_3H_3(H_{31}-D)^2 \\ & - \left[\frac{E_2H_2}{2}(H_{21}-D) + E_3H_3(H_{31}-D)\right]\left(\frac{H_{31}-D}{1+g}\right) \end{aligned} \tag{4}$$

where

$$D = \frac{E_2H_2(H_{21} - H_{31}/2) + g(E_2H_2H_{21} + E_3H_3H_{31})}{E_1H_1 + E_2H_2/2 + g(E_1H_1 + E_2H_2 + E_3H_3)}$$

$$H_{31} = \frac{(H_1 + H_3)}{2} + H_2$$

$$H_{21} = \frac{(H_1 + H_2)}{2} + H_2, \quad g = \frac{G_2}{E_3H_3H_2p^2}$$

E is Young's modulus of elasticity, G is the shear

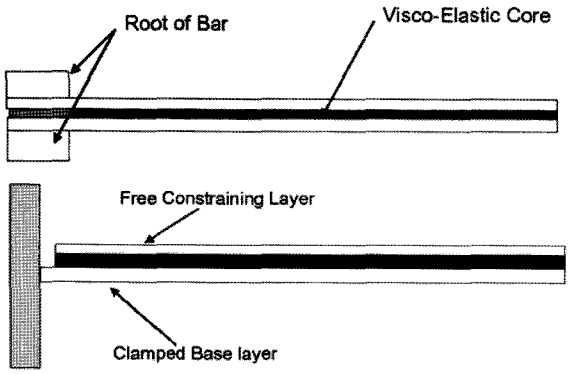

Figure 2. ASTM E756 (Top) & SAE J1637 (Bottom) Oberst Bar Configuration.

modulus, I is the second moment of area, H is the thickness, p is wave number, D is the distance from the neutral axis of the three layer system to that of the original beam, g is the shear parameter. Subscript 1 refers to the base structure, subscript 2 to the damping layer, subscript 3 to the constraining layer, and no subscript refers to the composite system.

To analyze the unconstrained layer damping treatment, it is necessary to consider the case for which the constraining layer thickness, H_3, is zero. And it is necessary to replace the terms given in that all E values and g by a complex modulus, $X(1+i\eta)$ in equation (4). Equating the real and imaginary parts, and noting that for all practical situations $(e_2h_2)^2 << e_2h_2$, the following two equations (5) can be derived:

$$\frac{EI}{E_1I_1} = \frac{1+4e_2h_2+6e_2h_2^2+4e_2h_2^3+e_2^2h_2^4}{1+e_2h_2}$$
$$\frac{\eta}{\eta_2} = \frac{e_2h_2(3+6h_2+4h_2^2+2eh_2^3+e_2^2h_2^4)}{(1+e_2h_2)(1+4e_2h_2+6e_2h_2^2+4e_2h_2^3+e_2^2h_2^4)} \quad (5)$$

where

$e_2 = E_2/E_1, \quad h_2 = H_2/H_1,$

The real part is used to compute the frequency, whereas the imaginary part is used to predict the damping performance.

4. FINITE ELEMENT MODELING

4.1. Detailed Model (Solid Element)

Each layer (H_1=0.8, H_2=0.8, H_3=0.07 mm) of sandwiched Oberst bar among bar specimens was represented by 3D solid element (CHEXA) and then viscoelastic properties given by modified ASTM equations in Table 1 were substituted in the model.

The same boundary condition as ASTM E756 was imposed on the FE model and unit force, in the out of plane direction, was defined to run the frequency response analysis.

Table 1. Viscoelastic material properties. (ρ=2160 kg/m^3)

Frequency (Hz)	G_v (Pa)	η_v
18 Hz	6.67E+0	0.01
127 Hz	7.70E+5	0.23
354 Hz	5.70E+5	0.71

Table 2. Equivalent material properties.

Frequency (Hz)	G (Pa)	f (Hz)	η
18 Hz	8.07E+9	17.96	0.05
127 Hz	9.89E+9	127.36	0.12
354 Hz	8.87E+9	354.18	0.18

The frequency and temperature dependent material properties of viscoelastic core should be reiterated over each interest frequency band for frequency response analysis. To reduce the number of iterations, this study was simplified by considering properties only at room temperature (20°C).

4.2. Equivalent Model (Single Shell Element)

After a MATLAB program was coded to calculate the RKU equations, a bar specimen (180×20 mm) was readily modeled by using shell element (CQUR4) and then the equivalent properties given in Table 2 were substituted in the model. One can use SDAMPING card and relevant dynamic load tabular function card (TABLED1) and modal damping table card (TABDMP1) implemented in MSC/NASTRAN to define stiffness and loss factor for the composite structures (Joseph, 1974; Lee, 2004; MSL, 1995). Boundary conditions and loading were kept the same as that for the detailed model.

Such a simplified approach does not increase the number of active degree of freedoms in the model, hence its result of numerical method represents a higher

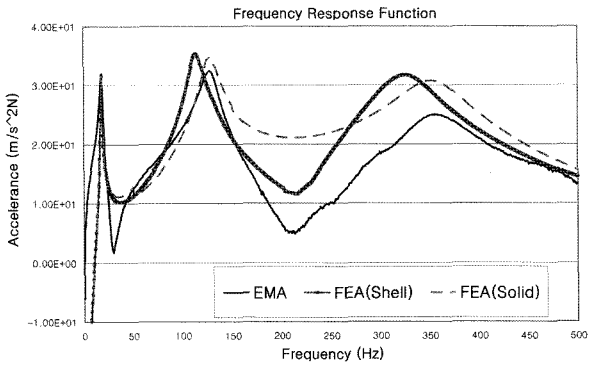

Figure 3. Comparative frequency response function (FEA/Equivalent model vs. EMA).

efficiency.

4.3. Comparison with Experiments

Frequency response function (FRF) from experimental modal analysis (EMA) was compared to that of the equivalent FEA models as shown in Figure 3.

FRFs at lower frequency range are more approximate than those at higher frequency range. Since the equivalent properties of constrained layer damping treatment that are assigned at the elemental level are determined by using the bending wave number, as a result, error may gradually increase.

5. AUTOMOTIVE APPLICATIONS

5.1. Simple Plates

As shown in Figure 4, viscoelastic patch is attached to the clamping part (Case 1) or the center part (Case 2) and then EMA and FEA for both cases are carried out.

The modal element strain energy of the aluminum plate with viscoelastic patch was calculated to understand the dynamic characteristics of the structure as a kind of standard. When each element strain energy of full structure was analyzed, as shown in Figure 5, it could be appeared that the modal strain energy was excessively distributed to clamping region in lower modes, whereas in higher modes to free end and to center part. As a result of this consideration, the locations of viscoelastic patches were selected at those regions (Johnson and Kienholz, 1982).

The element region which has especially large strain energy in accordance with each mode represents the location where the elastic strain is large. Accordingly, this affects directly relevant mode deflections (Johnson and Kienholz, 1983; Norton, 1989).

It is evident that FRF of Figure 6 measured by modal testing shows that Case 2 is more efficient for increasing damping benefit as compared with Case 1.

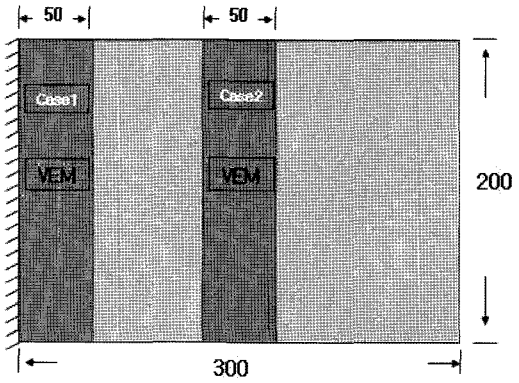

Figure 4. Configuration of the aluminum plate with viscoelastic patch.

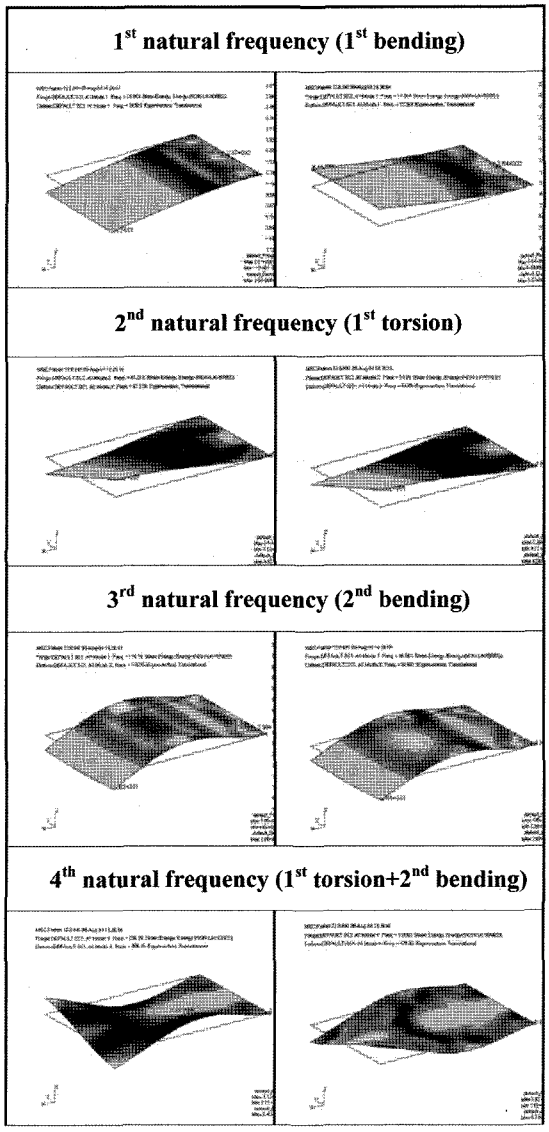

Figure 5. Distribution of the modal element strain energy (Case 1 vs. Case 2).

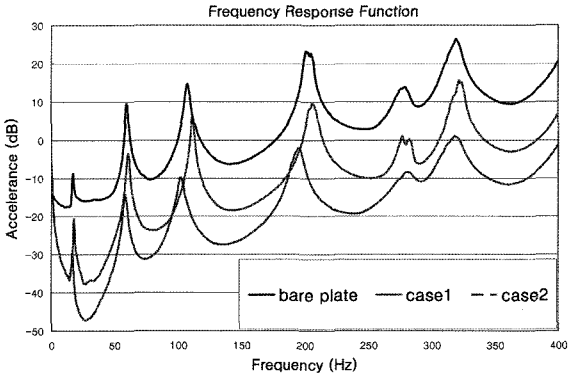

Figure 6. Comparison of experimental FRFs (bare plate, Case 1 vs. Case 2).

Table 3. Viscoelastic damping treatment in the Aluminum plate (Case 1).

Frequency (Hz)	EMA	FEA	Error (%)
1st	18.0	18.9	5.0
2nd	60.5	61.2	1.2
3rd	111.0	116.1	4.6

Table 4. Viscoelastic damping treatment in the Aluminum plate (Case 2).

Frequency (Hz)	EMA	FEA	Error (%)
1st	16.5	17.4	5.5
2nd	58.5	54.9	6.6
3rd	103.0	96.7	6.5

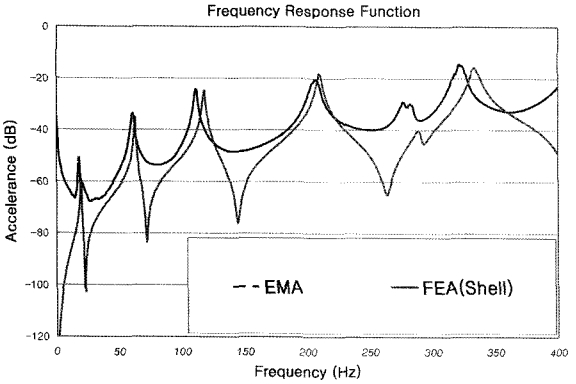

Figure 7. Comparison of FEA with EMA (Case 1).

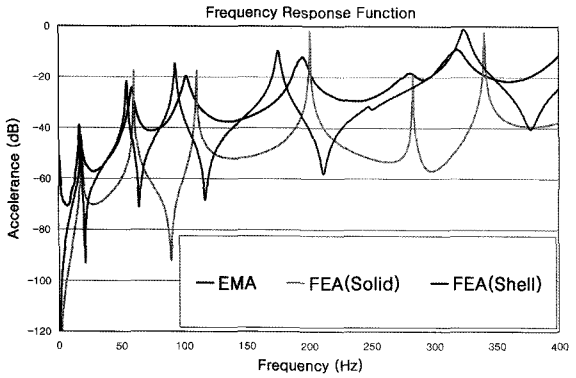

Figure 8. Comparison of FEA with EMA (Case 2).

The equivalent properties of the corresponding composite system according to each frequency range were substituted on the FE model, and then FEA was implemented by MSC/NASTRAN. As a result, it can be confirmed that experimental values and numerical values have a good agreement as given in Table 3 and Table 4.

When FRF of Case 2 as shown in Figure 8 which is

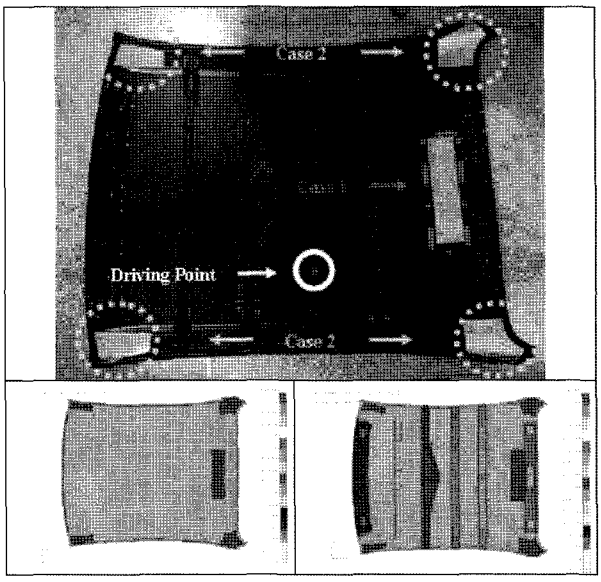

Figure 9. Position of the viscoelstic patches on th e roof compartment.

obtained through numerical analysis is examined, it can be seen that the peak values are relatively small as compared with Case 1 of Figure 7. Namely, it is more effective to control passively the higher mode in association with torsion for the strain energy against neutral plane of the element which it comes to get at the total of the element strain energy due to bending moment with the element strain energy owing to the coupling which is twisted. Moreover, the equivalent model (shell element) for computing the frequency response would be more reliable than the detailed model.

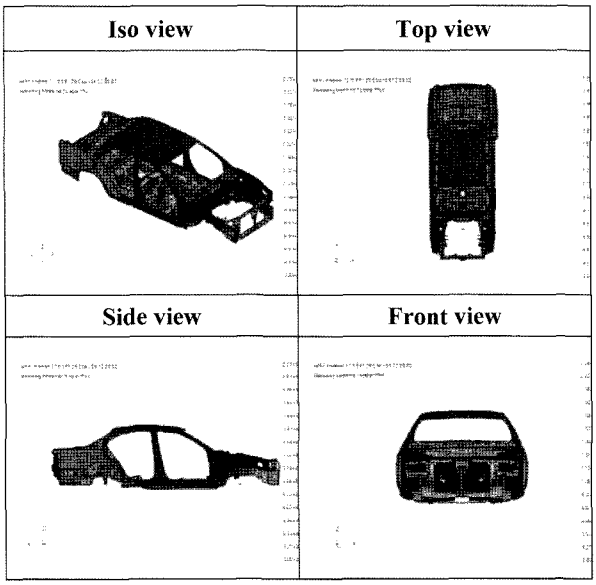

Figure 10. Vehicle body- in-white structure FE model.

BIW Structure		Roof Compartment	
Frequency (Hz)	Principal Motion	Frequency (Hz)	Principal Motion
30.8	1st Torsion	33.7	1st Bending
48.5	Torsion & Lateral	48.0	2nd Bending
49.9	2nd Bending		
52.4	3rd Bending		
		63.7	2nd Torsion
83.7		85.1	Torsion of Front
88.9	Local mode of Roof	91.2	Torsion of Rear
119	Local mode of Roof		

Figure 11. Comparison of natural frequencies (BIW) with natural frequencies (Roof).

5.2. Automotive Roof

On the basis of application to simple structure, the automotive steel roof (length 1480 mm, width 1130 mm, thickness 0.8 mm) with viscoelastic patches, as shown in Figure 9, was investigated to compare each FRF by EMA and FEA.

Roof structure in a full BIW model through the use of sets of three pillars (A, B and C pillar) has fully fixed boundary conditions by observing Figure 10. Whereas, free boundary conditions are imposed on the roof compartment. Broadly, the loss factors which can be obtained from the free boundary are almost the same as for fully fixed, but in the fundamental modes these may occur at different values of shear parameter (White, 1982).

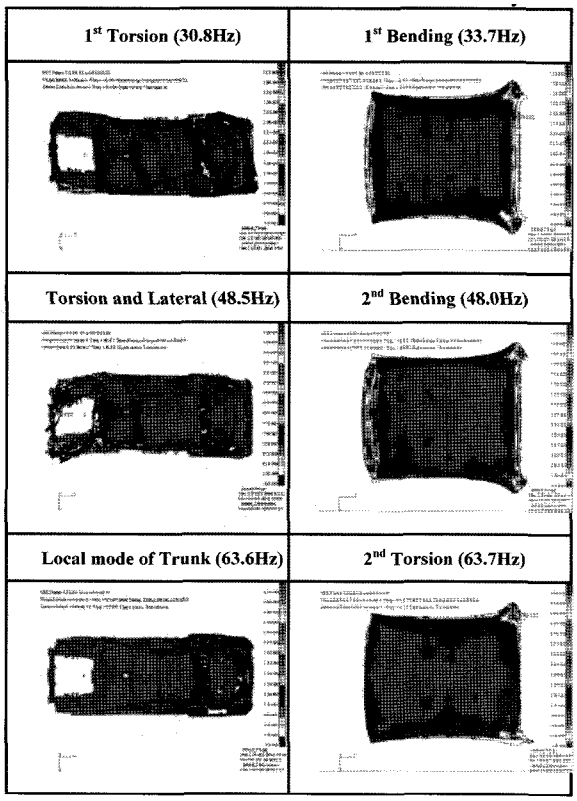

Figure 12. Distribution of the modal element strain energy (BIW structure vs. Roof compartment).

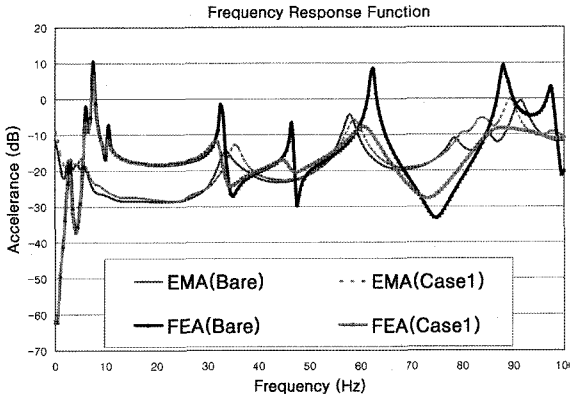

Figure 13. Comparison of FEA with EMA (Case 1).

Coupled main peaks of both BIW structure and roof compartment from FRF accomplished by dynamic analysis are obtained as shown in Figure 11. Therefore the corresponding positions of viscoelastic patch which follow the distribution of the strain energy along each other different boundary conditions are determined to accurately predict damping performance for the case of full vehicle application.

Figure 12 shows that the strain energy is concentrated on the front of rear roof-rail and on the both sides corner of rear roof at the below 100 Hz range and also is distributed intensively on the portion which is reinforced with the roof-rail at the above 100 Hz range. Especially, in the range 30 Hz to 90 Hz, the modal strain energy is extensively distributed on the center of roof.

The flexural loss factor and the flexural rigidity after

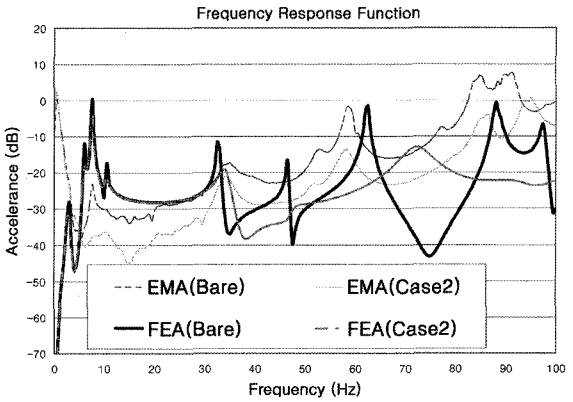

Figure 14. Comparison of FEA with EMA (Case 2).

and before the addition of the material all depend upon the wave number related to the real part of the flexural stiffness as well as on the shear modulus, G_2, of the damping layer. Therefore in contrast to the unconstrained layer damping, constrained layer damping does depend upon the mode of vibration. Besides, Figure 13 shows that there is very little shear strain in the damping layer and very little damping at very long wave lengths.

Compared to Case 1, Case 2 has relatively higher damping effect against main modes of BIW structure related the roof in the range 40–60 Hz and 80 Hz–110 Hz as given in Figure 14.

6. CONCLUSIONS

From the results for finite element analysis of constrained layer damping treatment, following conclusions have been obtained.

(1) The viscoelastic material has shear modulus of elasticity in the range 6.7E+3 to 7.7E+5 and loss factor in the range 0.01 to 0.71 for the frequency range of 10 Hz to 500 Hz.
(2) The loss factor of the damping layer depends upon the wave number as well as on the shear modulus.
(3) The viscoelastic material is best applied near vibrational antinodes rather than near stiffeners.
(4) It is more effective to govern the higher mode in relation to torsion rather than the lower mode in association with bending for passive constrained layer damping treatment.
(5) Higher computational efficiency is obtained to carry out frequency response analysis for the damped composite structure using the proposed equivalent modeling.
(6) Since the damping and flexural stiffness of the composite system depend upon the temperature of operation, on the damping layer thickness, on the extensional and flexural stiffness of the constraining layer and base structure as well as on the flexural wave number, the design for placement of viscoelastic patch and shape should be optimized by consideration of these things.

ACKNOWLEDGMENT–This study was supported by Brain Korea 21 Project in 2004.

REFERENCES

Akanda, A. and Goetchius, G. M. (1999). Representation of constrained/unconstrained layer damping treatments in FEA/SEA vehicle system models. *SAE Noise & Vibration Conf.*, Traverse City, MI.

Akanda, A. and Onsay, T. (2003). Material property characterization of foilback damping treatments using modified ASTM equations. *SAE Noise & Vibration Conf.*, Traverse City, MI.

American Society of Testing & Measurement Standards (ASTM) E 756 (1993).

Johnson, C. D. and Kienholz, D. A. (1982). Finite element prediction of damping in structures with constrained viscoelastic layers. *American Institute of Aeronautics and Astronautics J.* **20**, **9**, 1248–1290.

Johnson, C. D. and Kienholz, D. A. (1983). Prediction of damping in structures with viscoelastic materials. *MSC World User's Conf.*, Monterey, CA.

Joseph, J. A. (1974). (Ed.) *MSC/NASTRAN Applications Manual.* 2. MacNeal-Schwendler Corp.. Los Angeles. Calif.

Lee, K. (2004). Prediction of dynamic characteristics in vehicle body panels using an equivalent material properties of constrained layer damping treatment. *Spring Conf. Proc., Korean Society of Automotive Engineers*, 1183–1188.

Mead, D. J. (2000). *Passive Vibration Control.* John Wiley & Sons, Inc.. England. 388–409.

MSC/NASTRAN Advanced Dynamic User's Guide (1995). MacNeal-Schwendler Corp.. Los Angeles. CA.

MSC/NASTRAN Basic Dynamic User's Guide (1995). The MacNeal-Schwendler Corp.. Los Angeles. CA.

Nashif, A. D. (1985). *Vibration Damping.* John Wiley & Sons, Inc.. New York.

Norton, M. P. (1989). *Fundamentals of Noise and Vibration Analysis for Engineers.* Cambridge University Press. New York. 317–318.

Ross, D., Ungar, E. E. and Kerwin, E. M. Jr. (1959). *Damping of Plate Flexural Vibrations by Means of Viscoelastic Laminae.* Structural Damping, Section 3. ASME. New York.

Society of Automotive Engineers (SAE) Standards J-1637 (1993).

Wang, S. (1999). Simulation of beaded and curved panels with multi-layer damping treatment. *1st MSC Worldwide Automotive User Conf.*

White, R. G. (1982). *Noise and Vibration.* Ellis Horwood Ltd.. New York.